Nanoscale thermoelastic probing of megahertz thermal diffusion

Motonobu Tomoda[a] and Oliver B. Wright
Department of Applied Physics, Graduate School of Engineering, Hokkaido University, Sapporo, Hokkaido 060-8628, Japan

Roberto Li Voti
Dipartimento di Energetica, Università degli Studi di Roma "La Sapienza," Via A. Scarpa 16, 00161 Roma, Italy

(Received 21 June 2007; accepted 20 July 2007; published online 14 August 2007)

The authors demonstrate a method to probe thermal diffusion at megahertz frequencies with nanometer lateral resolution in a thin opaque film on a transparent substrate. They map photothermally induced megahertz surface vibrations in an atomic force microscope using tightly focused optical illumination from the substrate side. By comparison with a theoretical model of the surface displacement field, the authors derive the thermal diffusivity of a thin chromium film on a silica substrate. © *2007 American Institute of Physics*. [DOI: 10.1063/1.2770769]

With the continued trend for miniaturization of integrated circuit devices, there has been much interest in the thermal probing of thin films, multilayers, and microstructures down to nanometer length scales. The thermal properties of thin films are, in general, very different from the bulk and depend on defects, grain size, texture, and morphology.[1–3] Transient or sinusoidally modulated temperature fields are particularly useful for probing thermal properties because the associated thermal wave propagation can be accurately controlled or localized by choice of the time scale. For a modulation frequency f the thermal diffusion length decreases with increasing frequency as $1/f^{1/2}$, taking a value for metals that is typically ~ 1 μm for $f \approx 1$ MHz. Therefore, it is advantageous when probing thin films with thermal waves to work at high frequencies in order to restrict the measurement volume as much as possible to the film itself.

A particularly versatile noncontact method to transiently heat opaque thin films is to use pulsed or modulated optical beams, either focused to a single spot or crossed to produce induced gratings; time scales from seconds to picoseconds can be accessed in this way.[4–8] Likewise, optical detection of temperature fields by thermoreflectance or the mirage effect, or of surface displacement fields by optical beam deflection, interferometry, or diffraction have given rise to performant techniques for the noncontact probing of the thermal diffusivity in thin films.[8–13]

However, the lateral resolution of conventional optical detection methods is limited to micron scales owing to the optical diffraction limit. To overcome this limit for purposes of imaging transient thermal fields, the most developed thermal sensing schemes with submicron lateral resolution are based on scanned local probe techniques.[14,15] Use of a modulated heat source in an atomic force microscope (AFM) tip, for example, has proved useful for imaging time-varying temperature distributions up to frequencies of ~ 100 kHz.[15–17] AFM-based probing of kilohertz surface vibrations induced by resistive heating or chopped light allows additional contrast from the thermal expansion coefficient.[14,18]

Higher modulation frequencies in the megahertz range—more appropriate for probing thin films of thickness in the ~ 100 nm range or below—can be combined with nanometer spatial resolution using a method known as optical heterodyne force microscopy (OHFM).[19] This detects photothermally induced surface vibrations in an AFM, and can image subsurface nanoscale features through their effect on the surface displacement produced by a megahertz thermal field that is optically excited *directly below* the scanning AFM tip. To produce a quantitative measurement of the thermal diffusivity in thin films using the combination of megahertz thermal waves and local probing, however, one needs to move the scanning tip laterally with respect to the modulated thermal source in a way analogous to the conventional all-optical methods.[6,9,10]

In the present letter, we present a method based on OHFM to achieve this, involving optical excitation from the transparent substrate side of the sample and AFM detection of surface vibrations from the film side. We demonstrate the method using a thin Cr film on silica using variable frequency probing in the range of 100 kHz–4 MHz.

Figure 1 shows the modified OHFM setup. We use a commercial AFM system (TM microscopes, CP-M) based on an optical-lever detection system for the bending of a V-shaped cantilever (Ultralever D, length of 85 μm, width of 28 μm, thickness of 0.8 μm, spring constant of 1.6 Nm^{-1},

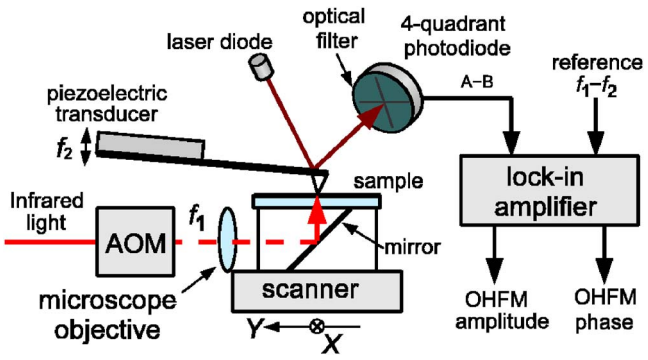

FIG. 1. (Color online) Schematic diagram of the modified optical heterodyne force microscope setup. AOM: acousto-optic modulator. The cantilever is slanted at an angle of 15° to the sample surface.

[a]Electronic mail: mtomoda@eng.hokudai.ac.jp

resonant frequency of 170 kHz, and tip radius of 10 nm). The sample consists of a polycrystalline Cr thin film with a thickness of 260 nm made by electron beam deposition on a fused silica substrate. The thickness was independently determined by laser picosecond acoustics.[20] An 830 nm laser beam chopped at a frequency $f_1 \sim 1$ MHz is focused on the substrate side of the Cr film through a 50× microscope objective lens, producing surface vibrations of small amplitude Δy (in the nanometer range) and phase ϕ through thermal expansion. The cantilever base is mounted on a piezoelectric slab that is excited at a slightly different frequency f_2 with an amplitude of ~1 nm. Because of the nonlinear nature of the tip-sample force-distance curve, a vibration of the contacting tip is induced at the difference frequency $f_1 - f_2 = 3$ kHz, chosen to be much lower than the fundamental cantilever resonance (~480 kHz in contact) but much higher than the response frequency of the AFM feedback loop (maintaining a set load of 30 nN). The amplitude (typically 20 pm here) and phase of the difference-frequency tip vibration is detected by a lock-in amplifier (with time constant 30 ms); as explained in more detail elsewhere,[19] the amplitude is proportional to Δy, whereas the phase should coincide with the phase ϕ of the surface displacement—apart from an additive constant that depends on the elastic properties of both tip and sample. For a sample with a homogeneous surface, one can therefore accurately probe the variations Δy and ϕ at f_1 through tip vibrations at the frequency $f_1 - f_2$ while maintaining a constant average distance between the tip and the sample.

The sample is mounted on a stage containing a mirror. This assembly, fixed to the AFM scanner, moves with respect to the tip. When the scanner moves in the Y direction parallel to the axis of the objective lens (see Fig. 1), the optical spot moves together with the sample. (In contrast, the spot moves across the sample surface when the scanner moves in the X direction perpendicular to this lens axis.) The amplitude and phase lag for scans along the Y axis across the center of the optical spot are recorded. The focus of the optical spot, with a full width at half maximum (FWHM) intensity $W = 1$ μm, is set when the tip is positioned at the center of the optical spot.[21]

Figure 2 shows Y-directed spatial scans of (a) the amplitude and (b) the phase lag of the difference-frequency signal (dots) for the optical chopping frequency $f_1 = 500$ kHz for an incident optical power $P = 1$ mW,[22] whereas (c) and (d) show the corresponding results for $f_1 = 2$ MHz and $P = 2$ mW, all data being obtained with a 2 μm s^{-1} scanning speed. (We estimate that $P = 1$ mW, equivalent to 0.6 mW absorbed power, results in a steady state temperature rise of 80 K at the Cr–SiO_2 interface, and an oscillating temperature change there at an amplitude of 40 K combined with a surface vibration amplitude of 0.12 nm at $f_1 = 500$ kHz.) The data are obtained by averaging the $+Y$ scans of 128×128 pixel raster-scanned images.

Immediately obvious from the data is a decrease in amplitude (becoming more pronounced at higher f_1) and an initial increase in phase lag as the tip position r deviates from the spot center ($r = 0$). For larger r the amplitude reaches a constant background governed by the noise level. The slight left-right asymmetry in the graphs is probably caused by residual heat conduction from the heated area through the air to the cantilever that is positioned to the left in Fig. 1.

To elucidate the detected signals, Fig. 2 also shows fits based on analytical calculations[23] of the amplitude and phase

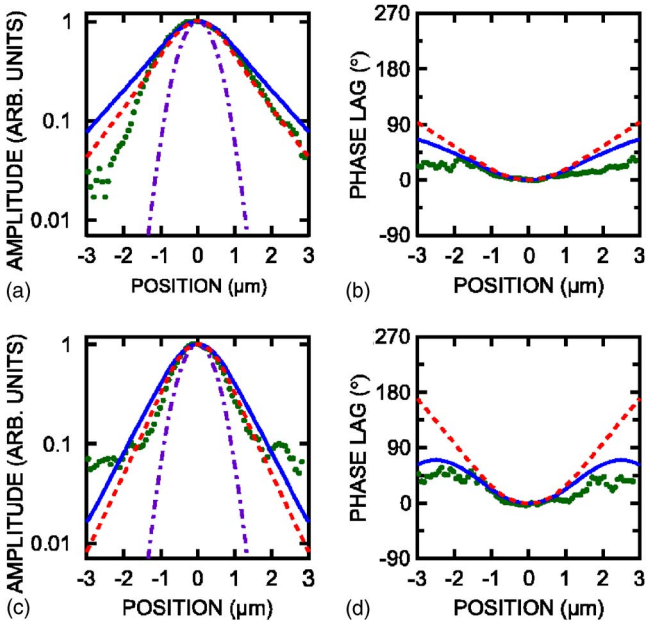

FIG. 2. (Color online) Measured amplitude and phase lag of the photothermally induced tip vibrations at $f_1 - f_2 = 3$ kHz, corresponding to a line scan (dots) across the spot center at [(a) and (b)] chopping frequency $f_1 = 500$ kHz with $P = 1$ mW and [(c) and (d)] $f_1 = 2$ MHz with $P = 2$ mW. Also shown are the calculated amplitudes and phase lag of the surface displacement (solid lines) and the surface temperature (dashed lines) at f_1, and the optical intensity profile (dotted-dashed lines).

of the surface temperature (dashed lines) and the surface displacement (solid lines). The theory, based on the use of thermoelastic potentials and a quasistatic thermal expansion, assumes a Gaussian optical spot profile (dotted-dashed lines) and a sinusoidally varying heat absorption (at f_1) at the interface. The geometry is a single isotropic layer on a semi-infinite isotropic substrate, and we ignore any thermal boundary resistance R_{th}.[24] First, the oscillating temperature field $T(x,y,z)$ is calculated, and then the surface displacement distribution $U(r)$ is obtained, where $r = (x^2 + y^2)^{1/2}$ is the radius to the surface detection point. As an aside, for the simpler case of a semi-infinite solid, $U(r)$ is a sum over volume elements dV' at $\mathbf{r}' = (x', y', z')$,

$$U(r) = \frac{(1+\nu)\alpha}{\pi} \int T(\mathbf{r}') \frac{z'}{|\mathbf{r} - \mathbf{r}'|^3} dV', \tag{1}$$

where ν is the Poisson ratio and α is the linear thermal expansion coefficient. (Nowacki[25] has derived a similar result for an infinite solid.) For our more complicated film-on-substrate geometry, the formulas are not reducible to a compact form such as Eq. (1). We take literature values for α, ν, shear modulus, and thermal diffusivity D_s of silica.[26–28] Likewise for Cr (Refs. 26 and 27) except the thermal diffusivity D_f because the thermal conductivities of thin films are known to differ strongly from bulk values. Using the data of Fig. 2 together with that of line scans at 100 kHz, 200 kHz, 1 MHz, and 4 MHz (not shown), we obtain $D_f = (4 \pm 2) \times 10^{-6}$ m^2 s^{-1} by least-square fitting to the phase and to the logarithm of the amplitude over regions (~±1.5 μm) of reasonable signal-to-noise ratio. The optical spot size $W = 1$ μm is taken directly from measurements with a knife edge. The derived value of D_f for Cr is seven times smaller than the corresponding bulk value.[26] This is not unexpected considering the effects of microstructure (inducing

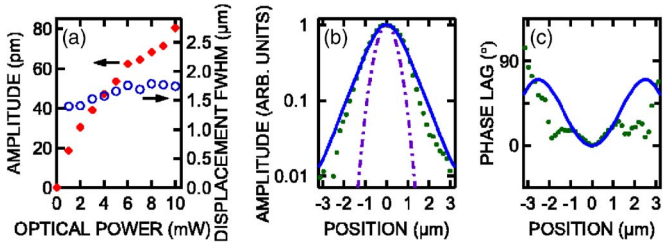

FIG. 3. (Color online) (a) Tip vibrational amplitude at $f_1-f_2=3$ kHz plotted (solid symbols) together with the FWHM of the amplitude-position curves (circles) vs incident optical power P for $f_1=2$ MHz. [(b) and (c)] Measured tip amplitude and phase lag profiles at 3 kHz (dots) at $f_1=2$ MHz and $P=8$ mW, and calculated amplitude and phase lag of the surface displacement (solid lines) at f_1 and spot profile (dotted-dashed lines).

grain-boundary scattering) or of contamination during sputtering (inducing impurity scattering).[29] Moreover, estimates based on van der Pauw electrical resistivity measurements[30] combined with the Wiedemann-Franz law[31] gave comparably reduced values for the thermal conductivity. The quality of the fits in Fig. 2 based on the fitted value of D_f is reasonable in the regions of significant signal.

The displacement amplitude varied linearly with the incident optical power up to 2 mW, but showed signs of saturation for higher powers, as shown in Fig. 3(a) for $f_1=2$ MHz. Interestingly, the FWHM width of the amplitude-position curves for displacement is not constant but increases with P [see Fig. 3(a)]. Such an increase, which compensates the amplitude saturation so that the product of FWHM width and amplitude [the product of the two curves in Fig. 3(a)] is approximately proportional to the absorbed power, may be due to the temperature dependence of the sample or tip physical properties, or of the water meniscus between the tip and the sample. Examples of Y-directed scans obtained at the relatively high power $P=8$ mW are shown in Figs. 3(b) and 3(c) for the amplitude and phase (dots), respectively. Because of the larger signal level, the signal-to-noise ratio is improved. The predicted amplitude and phase profiles for the displacement with the same value of D_f as above are also shown for reference. The agreement is still reasonable in spite of the nonlinear behavior.

At present our apparatus is restricted in application to one-dimensional spatial profiling because of the fixed tip and moving mirror stage setup. However, by using a scanned tip and a fixed stage it should be possible to obtain two-dimensional images of the thermoelastic field with nanoscale resolution. Since we are sensing surface displacement rather than temperature, the lateral resolution in the present setup is only limited by the mechanical contact area of nanometer order. Although it is difficult in arbitrary nanostructures to separate thermal diffusivity and thermal expansion, this method should prove useful for imaging nanoscale two-dimensional megahertz thermal fields in thin films and in nanostructures of well-defined geometry.

The authors are grateful to Osamu Matsuda for helpful discussions and to The Mazda Foundation for support. Part of the work was done in the framework of an agreement between the Japanese Society for the Promotion of Science and the Consiglio Nazionale delle Ricerche of Italy for the support of the mobility of researchers.

[1] D. G. Cahill, H. E. Fischer, T. Klitsner, E. T. Swartz, and R. O. Pohl, J. Vac. Sci. Technol. A **7**, 1259 (1989).
[2] J. C. Lambropoulos, M. R. Jolly, C. A. Amsden, S. E. Gilman, M. J. Sinicropi, D. Diakomihalis, and S. D. Jacobs, J. Appl. Phys. **66**, 4230 (1989).
[3] K. E. Goodson and M. I. Flik, Appl. Mech. Rev. **47**, 101 (1994).
[4] J. Opsal, A. Rosencwaig, and D. L. Willenborg, Appl. Opt. **22**, 3169 (1983).
[5] C. A. Paddock and G. L. Eesley, J. Appl. Phys. **60**, 285 (1986).
[6] E. P. Visser, E. H. Versteegen, and W. J. P. van Enckevort, J. Appl. Phys. **71**, 3238 (1992).
[7] O. W. Kading, H. Skurk, A. A. Maznev, and E. Matthias, Appl. Phys. A: Mater. Sci. Process. **61**, 253 (1995).
[8] S. Dilhaire, D. Fournier, and G. Tessier, in *Microscale and Nanoscale Heat Transfer*, Topics in Applied Physics Vol. 107, edited by S. Volz (Springer, Berlin, 2007), p. 239.
[9] B. Li, L. Pottier, J. P. Roger, D. Fournier, and E. Welsch, Rev. Sci. Instrum. **71**, 2154 (2000).
[10] W. B. Jackson, N. M. Amer, A. C. Boccara, and D. Fournier, Appl. Opt. **20**, 1333 (1981).
[11] E. Welsch and M. Reichling, J. Mod. Opt. **40**, 1455 (1993).
[12] Q. Shen, A. Harata, and T. Sawada, Jpn. J. Appl. Phys., Part 1 **35**, 2339 (1996).
[13] J. Jumel, F. Taillade, and F. Lepoutre, Eur. Phys. J.: Appl. Phys. **23**, 217 (2003).
[14] A. Majumdar, Annu. Rev. Mater. Sci. **29**, 505 (1999).
[15] H. M. Pollock and A. Hammiche, J. Phys. D **34**, R23 (2001).
[16] O. Kwon, L. Shi, and A. Majumdar, J. Heat Transfer **125**, 156 (2003).
[17] S. Lefèvre and S. Volz, Rev. Sci. Instrum. **76**, 033701 (2005).
[18] J. Bolte, F. Niebisch, J. Pelzl, P. Stelmaszyk, and A. D. Wieck, J. Appl. Phys. **84**, 6917 (1998).
[19] M. Tomoda, N. Shiraishi, O. V. Kolosov, and O. B. Wright, Appl. Phys. Lett. **82**, 622 (2003).
[20] O. B. Wright and K. Kawashima, Phys. Rev. Lett. **69**, 1668 (1992).
[21] We neglect the defocusing caused by scanner motion that gives rise to an estimated maximum 2% increase in W.
[22] We use subpicosecond optical pulses with 82 MHz repetition rate, but this has no influence on the sub-10 MHz dynamics here.
[23] R. Li Voti, O. B. Wright, and M. Tomoda (unpublished).
[24] Simulations showed that owing to the low substrate thermal diffusivity, the incorporation of any value of R_{th}, even infinite, changed the FWHM of the temperature profiles by $<10\%$ for a broad range of Cr diffusivities.
[25] W. Nowacki, *Thermoelasticity* (Pergamon, London, 1962), pp. 10–13.
[26] *American Institute of Physics Handbook*, 3rd ed., edited by D. E. Gray (McGraw-Hill, New York, 1972), pp. 3–107, 4–108, 4–135, 4–154, and 4–158.
[27] G. S. Kino, *Acoustic Waves: Devices, Imaging and Analog Signal Processing* (Prentice-Hall, New Jersey, 1987), p. 549.
[28] O. B. Wright, R. Li Voti, O. Matsuda, M. C. Larciprete, C. Sibilia, and M. Bertolotti, J. Appl. Phys. **91**, 5002 (2002).
[29] A. K. Kulkarni and L. C. Chang, Thin Solid Films **301**, 17 (1997).
[30] L. J. van der Pauw, Philips Res. Rep. **13**, 1 (1958).
[31] C. Kittel, *Introduction to Solid State Physics*, 7th ed. (Wiley, New York, 1996), pp. 166–168.